

# NONLINEAR SEQUENTIAL METHODS FOR IMPACT PROBABILITY ESTIMATION

Richard Linares\*, Puneet Singla<sup>†</sup> and John L. Crassidis<sup>‡</sup>

Orbit determination in application to the estimation of impact probability has the goal of determining the evolution of the state probability density function (pdf) and determining a measure of the probability of collision. Nonlinear gravitational interaction and non-conservative forces can make the pdf far from Gaussian. This work implements three nonlinear sequential estimators: the Extended Kalman Filter (EKF), the Unscented Kalman Filter (UKF) and the Particle Filter (PF) to estimate the impact probability. Both the EKF and the UKF make the Gaussian assumption and this work investigates the effect of this approximation on the impact probability calculation, while the PF can work for non-Gaussian systems.

## INTRODUCTION

After the formation of the early solar system some material failed to coalesce into planets, this mass became what is known as comets and asteroids. Most of this mass is held within the Kuiper belt and the Oort cloud and was believed to present no danger to Earth until a large scale computer simulation was performed to determine the time evolution of these objects. Through their natural evolution a few of these objects may have their orbits altered into trajectories that allow them to enter the Earth's neighborhood. Researchers found that asteroids in the main-belt in stable orbits are possible sources for Earth crossing asteroids.<sup>1</sup> These results indicated that an asteroid impacting with the Earth possesses a real threat to the planet and this threat must be anticipated and mitigated. Astronomers increase their searches for near-Earth objects (NEOs) and as a result the estimated numbers of NEOs dramatically expanded by about 1,000 times.<sup>2</sup> Although these objects are mostly composed of water ice with embedded dust particles and porous rocky cores, they can still possess a great danger to the Earth, having the potential of releasing large amount of energy upon impact.

The detection of asteroid 1989FC on March 23, 1989 made this threat real and brought NEOs to the public's attention. This asteroid was discovered only after it had a close approach to within 691,870 kilometers of the Earth, and this was determined only after backwards calculating the asteroid's orbit. This asteroid had kinetic energy of over 1,000 megaton hydrogen bombs.<sup>2</sup> Asteroid tracking and impact assessment then received federal funding and many more possible impactors have been detected, including 1997XF11, 1999AN10 and 1998 OX4, all of which had a finite probability of close-approach before being ruled out as impactors after tracking their path from

---

\*Graduate Student, Department of Mechanical & Aerospace Engineering, University at Buffalo, State University of New York, Amherst, NY. Email: linares2@buffalo.edu.

<sup>†</sup>Assistant Professor, Department of Mechanical & Aerospace Engineering, University at Buffalo, State University of New York, Amherst, NY. Email: psingla@buffalo.edu.

<sup>‡</sup>Professor, Department of Mechanical & Aerospace Engineering, University at Buffalo, State University of New York, Amherst, NY. Email: johnc@buffalo.edu.

sensor observations. The 99942 Apophis (2004 MN4) asteroid has received much attention after its initial discovery and is predicted to have a very close-approach in April 2029, where it will pass under some of our communication satellites. Although 2004 MN4 was initially predicted to have a nonzero probability of impact in 2029, later it was found to have little collision risk after further observation and analysis. In subsequent years 2004 MN4 is predicted to make close-approaches in 2034 and 2036. The impact probability associated with these approaches is difficult to compute due to the 2029 close encounter.

The calculation of an encounter probability involves three steps: determining an accurate orbit for the asteroid, confidence bounds for that orbit, and finally calculating the probability that at some time the confidence volume of the orbital position will intersect the planet of interest. Orbit determination is usually accomplished using a batch least squares approach which linearizes the dynamical system with respect to a nominal trajectory under the assumption that the true trajectory variation from the nominal one is small.<sup>3</sup> This assumption may be valid for some orbit determination applications but for anticipating possible NEOs this is not the case. In many cases an asteroid may be newly discovered or only observable for small portions of its orbit, therefore making the initial estimates of the orbit bad. Also since the orbital period of NEOs are on the order of several years there current track and any previous tracks may be widely separated. Close-approach times are usually years from the current measurement set. The nonlinear effect becomes even more apparent when propagating the orbit for long times into the future due to nonlinear gravitational interaction and non-conservative forces. This propagation is done by propagating the nominal orbit along with the covariance of the estimate error using a linearized variational equation (a first order state transition matrix).<sup>4</sup> Then the pdf at close approach is approximated by a Gaussian distribution which is completely described with the first order, “the mean,” and second order moments, “the covariance,” of the pdf. The pdf may be far from Gaussian due to nonlinear effects and the covariance propagation may also be far from linear, making this pdf a bad approximation.

The final task can be very complicated due to the time evolving nature of the relative orbits. We have some help here because we know that the  $N$  body effects during the time that the asteroid is in the sphere of influence of the Earth are very small, therefore we can consider the asteroid to be under pure two body Keplerian motion in this region. In Keplerian motion there are two quantities that are conserved, energy and specific angular momentum, and by applying these conservation equations to solve for the epoch state that results in an apogee distance less than the Earth’s radius approximate solution can be found. A transformation can be derived that maps from the state on the sphere of influence to the apogee space named the target plane.<sup>5</sup> The pdf is then integrated over a disk on the target plane representing apogee distances less than the effective radius of the Earth. This transformation is nonlinear and for large variation in initial condition the linearization can be invalid. The most accurate nonlinear approaches implement Monte Carlo sampling to space the pdf over a volume containing most of the probability mass. This can be very computationally expensive because the volume that contains most of the probability mass may be very large and the samples must fill the six dimensional state space.

The initial application of linear theory for close approach uncertainty and impact probability was to calculate Shoemaker-Levy 9 close-approaches to Jupiter by Chodas and Yeomans.<sup>6</sup> Linear methods were inadequate to analyze the collision probability of 1997XF close-approaches using initial observations due to strong nonlinearities introduced by a 2028 close-approach. Although later observation of 1997XF in 1990 ruled out any future impact, the hypothetical case of 1997XF before the 1990 observations was studied by two groups. Chodas and Yeoman applied a Monte

Carlo approach to estimate the impact probability,<sup>7</sup> where they sampled the initial distribution and integrated these samples up to close approach to calculate an impact probability. Milani developed a method called the Line of Variation (LOV) search,<sup>8</sup> where he sample the line of weakness in the initial condition and integrated this for the time span of interest. Both studies achieved similar results in calculating an impact probability of  $10^{-5}$  for the year 2040.

In many orbit determination applications the goal may be to determine an estimate for the orbit that is statistically consistent with all the available measurements, and therefore the estimator must provide an estimate and error bounds for that estimate. Orbit determination in application to estimating the impact probability on the other hand has a very different goal. The goal here is to determine the evolution of the pdf of the asteroid's state and determine a measure of the probability of collision. Therefore modeling the entire distribution is important. For this purpose, we compare three well-known filtering techniques: the Extended Kalman Filter (EKF), the Unscented Kalman Filter (UKF) and the Particle Filter (PF). The goal is to analyze the benefit that UKF and PF can provide over linear methods (EKF). Although the EKF and UKF assume the state pdf to be Gaussian, the UKF uses the full nonlinear model to compute the mean and state error covariance whereas the EKF uses a linearized dynamical model.

The organization of this paper is as follows. First, the system model for orbital dynamics and the target plane transformation are both discussed. Then, a description of the uncertainty modeling problem is given. Next, a review of the three filter solutions is provided. Finally, simulation results are shown for an impactor scenario where orbital initial uncertainty is considered to be the same for all three filters. Then the uncertainty is propagated and used to calculate the impact probability using the three filtering approaches.

## SYSTEM MODEL

### Orbital Dynamics

In this paper we will use the heliocentric position  $\mathbf{r}$  and velocity  $\mathbf{v}$  to represent the asteroid's state. The Newtonian  $N$  body gravitational equations of motion in heliocentric coordinates is given as:

$$\ddot{\mathbf{r}}_{s|a} = -\frac{\mu_s}{\|\mathbf{r}_{s|a}\|^3}\mathbf{r}_{s|a} - \sum_{i=1}^{N_p} \mu_i \left( \frac{\mathbf{r}_{s|a} - \mathbf{r}_{i|a}}{\|\mathbf{r}_{s|a} - \mathbf{r}_{i|a}\|^3} - \frac{\mathbf{r}_{s|a}}{\|\mathbf{r}_{s|a}\|^3} \right) + \mathbf{a}_D \quad (1)$$

where  $\mathbf{r}_{s|a}$  is the asteroid's position relative to the Sun,  $\mathbf{r}_{i|a}$  is the asteroid's position with respect to the  $i^{\text{th}}$  perturbing body and  $\mathbf{a}_D$  represents the perturbative accelerations. The terms  $\mu_s$  and  $\mu_i$  represent the gravitational parameters of the Sun and the  $i^{\text{th}}$  perturbing body, respectively. The term  $N_p$  represents the number of perturbing bodies, which include perturbations from the eight planets, Pluto and the three largest asteroids, Ceres, Pallas, and Vesta. An analytic solution to Eq. (1) including all the perturbations is not possible and therefore a numerical solution are used. For simplicity let  $\boldsymbol{\rho}_i = \mathbf{r}_{s|a} - \mathbf{r}_{i|a}$ , where  $\boldsymbol{\rho}_i = [\rho_{x_i}, \rho_{y_i}, \rho_{z_i}]^T$ .

### Target Plane Analysis

Consider a nominal orbit with initial conditions  $\mathbf{x}_o$ , where this initial condition has a close-approach with a planet at some time  $t^*$ . In practice, for planetary encounters, this close-approach distance is assumed to be between 0.03 and 0.1 AU.<sup>8</sup> Given that a close-approach can be identified, the initial conditions can be propagated to within the close-approach distance where the trajectory

can be well approximated by two body dynamics. At the point of closest-approach we define the close-approach distance as  $a_{CA}$ , where the subscript  $AC$  denotes close-approach. At this point the asteroid has a velocity  $v_{AC}$ . Note that if there is to be an encounter  $a_{AC} > R_e$  where  $R_e$  is the Earth radius. Near the Earth the trajectory interaction with all other body besides the Earth is small and therefore we approximate the dynamics to be two body near the Earth. Then the trajectory can be divided into two regions, the  $N$  body trajectory outside the Earth sphere of influence governed by Eq. (1) and a two body trajectory inside the Earth sphere of influence governed by two body dynamics. Our goal is to relate the apogee distance, for the two body trajectory (i.e. closest approach distance), to an impact parameter given any initial velocity and position within the Earth sphere of influence. Under pure two body dynamics there exists simple momentum and energy relations that can allow us to accomplish this. We begin by defining the relative-Earth state vectors  $\mathbf{x}_i = [\mathbf{r}_i^T \ \mathbf{v}_i^T]^T$ , where  $\mathbf{x}_i = \mathbf{x}_{s|a} - \mathbf{x}_{e|a}$  using the notation defined in Eq. (1). This vector is considered to be the state of an asteroid when it enters the Earth's sphere of influence with respect to the Sun.

Once in the sphere of influence, the orbit of an asteroid can be very well approximated by two body dynamics (assuming high relative velocity). We can define  $\mathbf{x}_{AC} = [\mathbf{r}_{AC}^T \ \mathbf{v}_{AC}^T]^T$ , the relative-Earth state vector, at the point of close approach as predicted by two body dynamics. Then by conservation of angular momentum we have

$$\mathbf{r}_i \times \mathbf{v}_i = \mathbf{r}_{AC} \times \mathbf{v}_{AC} \quad (2)$$

Since the velocity at closet approach is perpendicular to the position vector, Eq. (2) can be written in terms of perpendicular distances resulting in the following:

$$\boldsymbol{\delta} \times \mathbf{v}_i = \mathbf{a}_{AC} \times \mathbf{v}_{AC} \quad (3)$$

where  $\boldsymbol{\delta}$  is the perpendicular vector associated with  $\mathbf{r}_i$  and  $\mathbf{a}_{AC}$  is the perpendicular vector associated with  $\mathbf{r}_{AC}$ . The escape velocity,  $v_E$ , of the asteroid from  $a_{AC}$  to  $\mathbf{r}_i$  can be written using conservation of energy and is given by

$$v_E^2 = 2GM \left( \frac{1}{a_{AC}} - \frac{1}{D} \right) \quad (4)$$

where  $D = \|\mathbf{r}_i\|$  is the magnitude of  $\mathbf{r}_i$ . From conservation of energy, the initial velocity can be related to  $v_{AC}^2$  by  $v_{AC}^2 = v_E^2 + v_i^2$ , where  $v_i = \|\mathbf{v}_i\|$ . Then by substituting this into Eq. (3), the perpendicular distance can be written as

$$\delta = a_{AC} \sqrt{1 + \frac{v_i^2}{v_E^2}} \quad (5)$$

where  $\delta = \|\boldsymbol{\delta}\|$  is the magnitude of  $\boldsymbol{\delta}$ . The critical distance on the target plane where an encounter will occur is where  $a_{AC} > R_e$ , so therefore  $a_{AC} = R_e$  solves for the  $b$  plane or impact parameter  $b_e$ :

$$b_e = R_e \sqrt{1 + \frac{v_i^2}{v_E^2}} \quad (6)$$

where  $v_E^2 = 2GM \left( \frac{1}{a_p} - \frac{1}{D} \right) \approx 2GM(1/R_e)$  when  $R_e \ll D$ . The term  $b_e$  represents the minimum distance in the target plane where an encounter will occur. By integrating the probability

density function represented on the target plane over a disk with radius  $b_e$  centered at the Earth, the encounter probability can be calculated.

The choice of the target plane coordinate system is arbitrary, we label this coordinate system  $(\hat{e}_1, \hat{e}_2, \hat{e}_3)$ . The  $\hat{e}_3$ -axis is orientated in the direction of the geocentric velocity of the asteroid, and a convenient choice of the  $(\hat{e}_1, \hat{e}_2)$  directions is such that the  $\hat{e}_1$ -axis is aligned with the nominal target plane coordinate and the  $\hat{e}_2$ -axis is selected such that coordinate system is positively orientated.

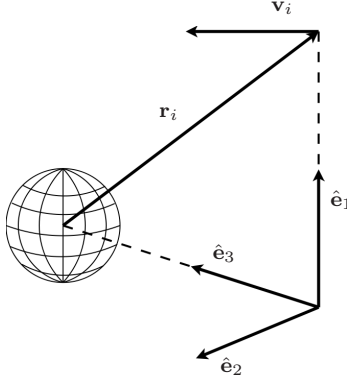


**Figure 1. Target Plane Geometry**

Using this coordinate system, there exists an orthogonal transformation matrix  $C$  that maps the original coordinate system into this new set of unit vectors such that

$$\begin{Bmatrix} \hat{e}_1 \\ \hat{e}_2 \\ \hat{e}_3 \end{Bmatrix} = \begin{bmatrix} C_{11} & C_{12} & C_{13} \\ C_{21} & C_{22} & C_{23} \\ C_{31} & C_{32} & C_{33} \end{bmatrix} \begin{Bmatrix} \hat{i} \\ \hat{j} \\ \hat{k} \end{Bmatrix} \quad (7)$$

The coordinate systems can be aligned by two rotation matrices given by the following expression

$$\begin{Bmatrix} \hat{e}_1 \\ \hat{e}_2 \\ \hat{e}_3 \end{Bmatrix} = \begin{bmatrix} \cos(\lambda) & 0 & \sin(\lambda) \\ 0 & -1 & 0 \\ -\sin(\lambda) & 0 & \cos(\lambda) \end{bmatrix} \begin{bmatrix} \cos(\theta) & \sin(\theta) & 0 \\ -\sin(\theta) & \cos(\theta) & 0 \\ 0 & 0 & -1 \end{bmatrix} \begin{Bmatrix} \hat{i} \\ \hat{j} \\ \hat{k} \end{Bmatrix} \quad (8)$$

where  $\theta$  and  $\lambda$  are the angles giving the orientation of the  $v_i$  vector. The vectors  $\{\hat{i}, \hat{j}, \hat{k}\}$  are the coordinate axis of the inertial frame. The target plane coordinates are  $\delta = [\delta_1, \delta_2]^T$ ; then a transformation that maps from the inertial to the target plane can be written as

$$T(\theta, \lambda) = \begin{bmatrix} 0 & 1 & 0 \\ 0 & 0 & 1 \end{bmatrix} \begin{bmatrix} \cos(\lambda) & 0 & \sin(\lambda) \\ 0 & -1 & 0 \\ -\sin(\lambda) & 0 & \cos(\lambda) \end{bmatrix} \begin{bmatrix} \cos(\theta) & \sin(\theta) & 0 \\ -\sin(\theta) & \cos(\theta) & 0 \\ 0 & 0 & -1 \end{bmatrix} \quad (9)$$

Carrying out the matrix multiplication we can write the final form of the target plane transformation as

$$T(\theta, \lambda) = \begin{bmatrix} -\sin(\theta) & \cos(\theta) & 0 \\ -\cos(\theta)\sin(\lambda) & \sin(\theta)\sin(\lambda) & \cos(\lambda) \end{bmatrix} \quad (10)$$

Using the definition of the target plane coordinate vector  $\boldsymbol{\delta}$ , and  $\mathbf{v} = [v_x, v_y, v_z]^T$  we can write the target plane vector in terms of initial condition  $\mathbf{x} = [\mathbf{r}^T \ \mathbf{v}^T]^T$ :

$$\boldsymbol{\delta} = T(\theta, \lambda)\mathbf{r} \quad (11a)$$

$$\lambda = \tan^{-1} \left( \frac{v_z}{\|\mathbf{v}\|} \right) \quad (11b)$$

$$\theta = \sin^{-1} \left( \frac{v_y}{\sqrt{v_x^2 + v_y^2}} \right) \quad (11c)$$

The following notation will be used for the target plane transformation henceforth:

$$\boldsymbol{\delta} = \mathbf{B}(\mathbf{x}) = T(\theta, \lambda)\mathbf{r} \quad (12)$$

Once the target plane transformation has been defined given an initial condition of a possible impactor, one propagates the heliocentric state vector until close approach distance (within the Earth's sphere of influence) and then applies the target plane transformation. The target plane coordinate is then used to determine whether or not there will be an impact, if the coordinate  $\boldsymbol{\delta}$  is within a disk of radius  $b_e$  there will be an impact with the earth. This approach gives a yes-no answer to whether there will be an impact; but what if we have not one initial condition but a distribution of initial conditions? This would be a distribution representing the knowledge about the state of the asteroid. In the following sections three methods for modeling this distribution and applying the target plane transformation are discussed.

## UNCERTAINTY

A mechanism to represent the uncertainty is necessary before the model data and the sensor data can be integrated in an efficient and consistent manner. Probabilistic means of representing uncertainties have been explored extensively and provide the greatest wealth of knowledge which can be exploited in this work. In the following section we will review uncertainty modeling using a probabilistic approach.

### Uncertainty Representation

In conventional deterministic systems, the system state assumes a fixed value at any given instant of time. However, in stochastic dynamics it is a random variable and its time evolution is given by a stochastic differential equation:

$$\dot{\mathbf{x}} = \mathbf{f}(\mathbf{x}, t) + \mathbf{g}(t, \mathbf{x})\boldsymbol{\Gamma}(t) \quad (13)$$

where  $\boldsymbol{\Gamma}(t)$  represents a Wiener process with the correlation matrix  $\mathbf{Q}$ . The uncertainty associated with the state vector  $\mathbf{x}$  is usually characterized by time parameterized state pdf  $p(t, \mathbf{x})$ . In essence, the study of stochastic systems reduces to finding the nature of such time-evolution of the system-state pdf described by the following pde, known as the Fokker-Planck-Kolmogorov Equation (FPKE):

$$\mathcal{L}_{\mathcal{FP}}[p(t, \mathbf{x})], \quad \mathcal{L}_{\mathcal{FP}} = \left[ - \sum_{i=1}^n \frac{\partial}{\partial x_i} D_i^{(1)}(t, \mathbf{x})[\cdot] + \sum_{i=1}^n \sum_{j=1}^n \frac{\partial^2}{\partial x_i \partial x_j} D_{ij}^{(2)}(t, \mathbf{x})[\cdot] \right] \quad (14)$$

where  $\mathbf{D}^{(1)}$  is known as the Drift Coefficient, which  $\mathbf{D}^{(2)}$  is called the *Diffusion Coefficient* and are given by the following equations:

$$\mathbf{D}^{(1)}(t, \mathbf{x}) = \mathbf{f}(t, \mathbf{x}) + \frac{1}{2} \frac{\partial \mathbf{g}(t, \mathbf{x})}{\partial \mathbf{x}} \mathbf{Q} \mathbf{g}(t, \mathbf{x}), \quad \mathbf{D}^{(2)}(t, \mathbf{x}) = \frac{1}{2} \mathbf{g}(t, \mathbf{x}) \mathbf{Q} \mathbf{g}^T(t, \mathbf{x}) \quad (15)$$

The FPKE is a formidable problem to solve, because of the following issues: 1) *Positivity* of the pdf, 2) *Normalization* constraint of the pdf:  $\int_{\mathbb{R}^n} p(t, \mathbf{x}) d\mathbf{x} = 1$ , and 3) *No fixed Solution Domain*: how to impose boundary conditions in a finite region and restrict numerical computation to regions where  $p > \sim 10^{-9}$ .

Analytical solutions for the FPKE exist only for a stationary pdf and are restricted to a limited class of dynamical systems.<sup>9</sup> Thus researchers are actively looking at numerical approximations to solve the FPKE,<sup>10,11</sup> generally using the variational formulation of the problem. However, these methods are severely handicapped for higher dimensions because the discretization of the space over which pdf lives is computationally impractical. Alternatively many approximate techniques exist in the literature to approximate the uncertainty evolution, the most popular being Monte Carlo (MC) methods,<sup>12</sup> Gaussian closure,<sup>13</sup> Equivalent Linearization,<sup>14</sup> and Stochastic Averaging.<sup>15</sup> All of these algorithms, except Monte Carlo methods, are similar in several respects, and are suitable only for linear or moderately nonlinear systems, because the effect of higher order terms can lead to significant errors. Monte Carlo methods require extensive computational resources and effort, and become increasingly infeasible for high-dimensional dynamic systems.

The use of sensor data to correct and refine the dynamical model forecast so as to reduce the associated uncertainties is a logical improvement over purely model-based prediction. However, mathematical models for various sensors are generally based upon the “usefulness” rather than the “truth” and do not provide all the information that one would like to know. This approach had its birth with the development of the Bayesian estimation.

Between two measurement time instants the procedure discussed in the last section can be used to propagate the weights, mean and covariance of different Gaussian components through the nonlinear dynamical system and whenever a measurement is available, Bayes rule can be used to update the conditional pdf:

$$p(\mathbf{x}_k | \mathbf{Y}_k) = \frac{p(\mathbf{y}_k | \mathbf{x}_k) p(\mathbf{x}_k | \mathbf{Y}_{k-1})}{\int p(\mathbf{y}_k | \mathbf{x}_k) p(\mathbf{x}_k | \mathbf{Y}_{k-1}) d\mathbf{x}_k} \quad (16)$$

This equation can be interpreted as follows: Let  $p(\mathbf{x})$  represent the prior belief of what values the random state vector  $\mathbf{x}$  might take (prior pdf usually obtained by propagating the initial pdf through the FPKE). We now observe from a sensor the measurement vector  $\mathbf{y}$  which is represented as a conditional pdf  $p(\mathbf{y} | \mathbf{x})$  which describes the likelihood that we observe  $\mathbf{y}$  given  $\mathbf{x}$ . We now need to determine the new posterior distribution function  $p(\mathbf{x} | \mathbf{y})$  of  $\mathbf{x}$  given the prior pdf  $p(\mathbf{x})$  and the information provided by the observation. The denominator term in Eq. (16) is essentially for normalizing such that the posterior distribution satisfies the constraints of a pdf.

The Bayesian approach has its birth with the development of the Kalman Filter<sup>16</sup> (KF). Subsequently various researchers have endeavored to exploit knowledge of statistics, dynamic systems and numerical analysis to develop techniques<sup>17,18,19</sup> which cater to the various classes of problems of interest. For low-order nonlinear systems, Particle filters<sup>18,19</sup> have been gaining increasing attention.

The goal is to determine  $\mathcal{P}r\{\|\mathbf{x}_t\| \leq R_e\}$  the probability that the state  $\mathbf{x}_t$  is within the region  $R_e$ . The following integral calculates the probability of collision given  $p(\mathbf{x}_t)$ :

$$\mathcal{P}r\{\|\mathbf{x}_t\| \leq R_e\} = \int \int_{\Omega} p(\mathbf{x}_t) d\mathbf{x} dt \quad (17)$$

where  $\Omega$  is the Earth's volume and the integral is over all time. The goal of this paper is to investigate three methods, the Extended Kalman Filter (EKF), the Unscented Kalman Filter (UKF) and the Particle Filter (PF) to evaluate this integral.

## APPROXIMATE METHODS: KALMAN FILTER APPROACH

The Kalman filter assumes that the posterior density  $p(\mathbf{x}_k | \mathbf{Y}_{1:k})$  is Gaussian for any  $k$ , where  $\mathbf{Y}_t$  is a realization of a sequence of observations  $\{\tilde{\mathbf{y}}_1, \dots, \tilde{\mathbf{y}}_t\}$  of the state of the system up to time  $t_k$  where  $t \geq t_k$ . Also the state  $\mathbf{x}$  at time  $t_k$  will be written as  $\mathbf{x}_k$ . This assumption holds conditioned that the density  $p(\mathbf{x}_{k-1} | \mathbf{Y}_{1:k-1})$  is Gaussian and that the observation function  $\mathbf{h}(\mathbf{x})$  is linear. Between observations the Kalman filter approximates the conditional density  $p(\mathbf{x}_k | \mathbf{Y}_{1:k-1})$  as a Gaussian distribution. This is valid if the process noise  $\mathbf{w}$  is Gaussian and the system model  $\mathbf{f}(\mathbf{x})$  is linear. Under these assumptions the Kalman filter forms a minimum variance estimator providing optimal estimates of the state based on the assumed statistical information about the dynamical and observation model. No unbiased estimator can do better than a Kalman filter in the very restrictive linear and Gaussian environment. In many situations, the linear assumptions on these functions may not hold. Therefore an approximate solution for the conditional density is necessary. The EKF uses a Kalman filter framework by performing a local linearization of  $\mathbf{f}(\mathbf{x})$  and  $\mathbf{h}(\mathbf{x})$  about the current estimate  $\mathbf{x}$  and assumes this describes the nonlinearity.

### Predictor

An EKF is now summarized for estimating the state of an asteroid position and velocity given by  $\mathbf{x} = [\mathbf{r}^T \ \mathbf{v}^T]^T$ . The standard orbit model in Eq. (1) can be written in the general state equation which gives us the deterministic part of our stochastic model:

$$\dot{\mathbf{x}} = \mathbf{f}(\mathbf{x}, t) + \mathbf{g}(\mathbf{x}, t) \mathbf{\Gamma}(t) \quad (18)$$

where  $\mathbf{\Gamma}(t)$  is a gaussian white noise process term with correlation function  $\mathbf{Q}\delta(t_1 - t_2)$ . The  $\mathbf{f}(\mathbf{x}, t)$  function is a general nonlinear function. To solve the general nonlinear filtering problem the EKF linearizes the function  $\mathbf{f}(\mathbf{x}, t)$  about the current nominal state. Then if the initial pdf  $p(\mathbf{x}_o)$  capturing the initial state uncertainty is given then the time evolution of  $p(\mathbf{x}, t)$  can be described by the FPKE in Eq. (14).

A linear mapping will transform a Gaussian into another Gaussian, where the parameters (mean and covariance) of the resulting distribution can be easily computed. But the outcome of a Gaussian that undergoes a nonlinear transformation is generally non-Gaussian. Conventionally, a Gaussian approximation to the forecast density function  $p(\mathbf{x}, t)$  is obtained by linearizing the nonlinear transformation and the propagation equations which can be written as

$$\dot{\boldsymbol{\mu}} = \mathbf{f}(\boldsymbol{\mu}, t) \quad (19a)$$

$$\dot{\mathbf{P}} = \mathbf{A}(\boldsymbol{\mu})\mathbf{P} + \mathbf{P}\mathbf{A}^T(\boldsymbol{\mu}) + \mathbf{g}(\boldsymbol{\mu}, t) \mathbf{Q}\mathbf{g}^T(\boldsymbol{\mu}, t) \quad (19b)$$

where

$$\mathbf{A}(\boldsymbol{\mu}) = \left. \frac{\partial \mathbf{f}(\mathbf{x}, t)}{\partial \mathbf{x}} \right|_{\mathbf{x}=\boldsymbol{\mu}} \quad (20)$$

Then the final approximated forecast density can be written as

$$p(\mathbf{x}, t) = \mathcal{N}(\boldsymbol{\mu}, \mathbf{P}) \quad (21)$$

Given the state equation is a the orbit model in Eq. (1), the Jacobian matrix of the state equation is given by

$$\mathbf{A}(\mathbf{x}) = \begin{bmatrix} 0_{3 \times 3} & I_{3 \times 3} \\ \mathbf{J}_{3 \times 3} & 0_{3 \times 3} \end{bmatrix} \quad (22)$$

and  $\mathbf{J}$  is a gravity gradient matrix which can be written by

$$\mathbf{J} = \mathbf{G} - \mathbf{K} \quad (23)$$

where

$$\mathbf{G} = \begin{bmatrix} -\frac{\bar{\mu}}{\|\mathbf{r}_s|a\|^3} + \frac{3\bar{\mu}x_s^2|a}{\|\mathbf{r}_s|a\|^5} & \frac{3\bar{\mu}x_s|a y_s|a}{\|\mathbf{r}_s|a\|^5} & \frac{3\bar{\mu}x_s|a z_s|a}{\|\mathbf{r}_s|a\|^5} \\ \frac{3\bar{\mu}y_s|a x_s|a}{\|\mathbf{r}_s|a\|^5} & -\frac{\bar{\mu}}{\|\mathbf{r}_s|a\|^3} + \frac{3\bar{\mu}y_s^2|a}{\|\mathbf{r}_s|a\|^5} & \frac{3\bar{\mu}y_s|a z_s|a}{\|\mathbf{r}_s|a\|^5} \\ \frac{3\bar{\mu}z_s|a x_s|a}{\|\mathbf{r}_s|a\|^5} & \frac{3\bar{\mu}z_s|a y_s|a}{\|\mathbf{r}_s|a\|^5} & -\frac{\bar{\mu}}{\|\mathbf{r}_s|a\|^3} + \frac{3\bar{\mu}z_s^2|a}{\|\mathbf{r}_s|a\|^5} \end{bmatrix} \quad (24a)$$

$$\mathbf{K} = \begin{bmatrix} \sum \left( \frac{-\mu_i}{\|\boldsymbol{\rho}_i\|^3} + \frac{3\mu_i \rho_{x_i}^2}{\|\boldsymbol{\rho}_i\|^5} \right) & \sum \mu_i \left( \frac{3\rho_{x_i} \rho_{y_i}}{\|\boldsymbol{\rho}_i\|^5} \right) & \sum \mu_i \left( \frac{3\rho_{x_i} \rho_{z_i}}{\|\boldsymbol{\rho}_i\|^5} \right) \\ \sum \mu_i \left( \frac{3\rho_{y_i} \rho_{x_i}}{\|\boldsymbol{\rho}_i\|^5} \right) & \sum \left( \frac{-\mu_i}{\|\boldsymbol{\rho}_i\|^3} + \frac{3\mu_i \rho_{y_i}^2}{\|\boldsymbol{\rho}_i\|^5} \right) & \sum \mu_i \left( \frac{3\rho_{y_i} \rho_{z_i}}{\|\boldsymbol{\rho}_i\|^5} \right) \\ \sum \mu_i \left( \frac{3\rho_{z_i} \rho_{x_i}}{\|\boldsymbol{\rho}_i\|^5} \right) & \sum \mu_i \left( \frac{3\rho_{z_i} \rho_{y_i}}{\|\boldsymbol{\rho}_i\|^5} \right) & \sum \left( \frac{-\mu_i}{\|\boldsymbol{\rho}_i\|^3} + \frac{3\mu_i \rho_{z_i}^2}{\|\boldsymbol{\rho}_i\|^5} \right) \end{bmatrix} \quad (24b)$$

where  $\bar{\mu} = (\mu_s - \sum \mu_i)$  is the sum of the gravitational parameter for each body.

### Corrector

Given a system model with initial state and covariance values, the EKF propagates the state vector and the error covariance matrix recursively. Then, along with imperfect measurements, the EKF updates the state and covariance matrix. The update is accomplished through the Kalman gain matrix  $\mathcal{K}$ , which is obtained by minimizing the weighted sum of the diagonal elements of the error covariance matrix. Thus, the EKF algorithm has a distinctive predictor corrector structure. The prediction phase is important for overall filter performance. In general, the discrete measurement equation can be expressed for the filter as

$$\tilde{\mathbf{y}}_k = \mathbf{h}(\mathbf{x}_k, t) + \mathbf{v}_k(t) \quad (25)$$

where  $\tilde{\mathbf{y}}_k$  is a measurement vector and  $\mathbf{v}_k(t)$  is a measurement noise which is assumed to be a white Gaussian noise process. The noise statistic of  $\tilde{\mathbf{y}}_k$  can be described completely by  $\mathbf{v}_k(t) \sim \mathcal{N}(\mathbf{0}, \mathbf{R}(t))$  where  $E\{\mathbf{v}_k(t)\} = \mathbf{0}$  and  $E\{[\mathbf{v}_k(t) - E\{\mathbf{v}_k(t)\}][\mathbf{v}_k(t) - E\{\mathbf{v}_k(t)\}]^T\} = \mathbf{R}(t)$  represents the covariance of  $\mathbf{v}_k(t)$ . To use a recursive filter, the EKF expresses the state and measurement equation in the linearized form. Using Bayes' theorem under the linear gaussian assumption we can

determine a relationship to update the mean and covariance of the distribution by minimizing the error covariance matrix, providing an optimal estimate of the state in a minimum variance sense. Then the following update equation can be written for the mean of the state distribution

$$\boldsymbol{\mu}_{k|k} = \boldsymbol{\mu}_{k|k-1} + \mathcal{K}_k [\mathbf{z}_k - \mathbf{h}(\boldsymbol{\mu}_{k|k-1})] \quad (26)$$

where the notation of superscripts  $(k|k-1)$  denote the estimate at the measurement update time which is conditioned on the previous measurements and has not been updated; the first  $k$  term represents the time step the estimate is given for and the second subscript represents the last time step the estimate was updated with measurements. The  $\mathcal{K}$  matrix is a gain at the measurement time update given by

$$\mathcal{K}_k = \mathbf{P}_{k|k-1} \hat{\mathbf{H}}(\boldsymbol{\mu}_{k|k-1})^T \left[ \hat{\mathbf{H}}(\boldsymbol{\mu}_{k|k-1}) \mathbf{P}_{k|k-1} \hat{\mathbf{H}}(\boldsymbol{\mu}_{k|k-1})^T + \mathbf{R}_k \right]^{-1} \quad (27a)$$

$$\mathbf{P}_{k|k} = \mathbf{P}_{k|k-1} - \mathcal{K}_k \hat{\mathbf{H}}(\boldsymbol{\mu}_{k|k-1}) \mathbf{P}_{k|k-1} \quad (27b)$$

where  $\mathbf{P}_{k|k}$  is an covariance matrix at  $k$  time step conditioned on the measurements up to the  $k^{\text{th}}$  time step and  $\hat{\mathbf{H}}(\boldsymbol{\mu}_{k|k-1})$  is given by:

$$\hat{\mathbf{H}}(\boldsymbol{\mu}_{k|k-1}) = \left. \frac{\partial \mathbf{h}(\mathbf{x}, t)}{\partial \mathbf{x}} \right|_{\mathbf{x}=\boldsymbol{\mu}} \quad (28)$$

The term  $\hat{\mathbf{H}}(\boldsymbol{\mu}_{k|k-1}) \mathbf{P}_{k|k-1} \hat{\mathbf{H}}(\boldsymbol{\mu}_{k|k-1})^T + \mathbf{R}_k$  is called the innovation covariance and it comes from the likelihood function, it represents the covariance of predicted state error,  $\mathbf{e} = \{\tilde{\mathbf{y}}_k - \mathbf{h}(\mathbf{x}_{k|k-1}, t)\}$ , assuming Gaussian distribution for  $\mathbf{x}_{k|k-1}$  and  $\tilde{\mathbf{y}}_k$ . While propagating the orbit if there is a measurement made available, Eq. (27a) and Eq. (27b) can be used to update the pdf of the state vector condition on all measurements that are available at the current time step. Therefore, given an orbit that has been determined and the uncertainty quantified using the Gaussian assumption, if further measurements are made available, Eq. (27a) and Eq. (27b) can be used to update the pdf and recalculate the probability of impact given these new measurements.

### Target Plane Approximation

The EKF approach to propagating uncertainty can be applied to the target plane transformation by linearizing the target plane transformation about the nominal state vector. Given the nonlinear target plan transformation in Eq. (10), the linear model can be written as

$$\boldsymbol{\mu}_\delta = \mathbf{F}(\boldsymbol{\mu}) \mathbf{x} \quad (29)$$

where

$$\mathbf{F}(\boldsymbol{\mu}) = \left. \frac{d\mathbf{B}(\mathbf{x})}{d\mathbf{x}} \right|_{\mathbf{x}=\boldsymbol{\mu}} \quad (30)$$

The quantity  $\boldsymbol{\mu}_\delta$  is the mean of the state on the target plane, which is an approximation for  $E\{\boldsymbol{\delta}\}$ . The matrix  $\mathbf{F}(\boldsymbol{\mu})$  is the Jacobian of target plane transformation evaluated at the mean, which can be determined by taking the derivative of Eq. (10) with respect to the state vector  $\mathbf{x}$  and setting  $\mathbf{x} = \boldsymbol{\mu}$ . The  $\mathbf{F}(\mathbf{x})$  matrix can be written as

$$\mathbf{F}(\mathbf{x}) = \left[ \begin{array}{cc} T(\theta, \lambda) & \frac{d\delta}{d\Theta} \frac{d\Theta}{dv^T} \end{array} \right] \quad (31)$$

where  $\Theta$  represents a vector of the angles  $\theta$  and  $\lambda$ ,  $\Theta = [\theta, \lambda]^T$ . Then the expression for  $\frac{d\delta}{d\Theta}$  can be shown to be

$$\frac{d\delta}{d\Theta} = \begin{bmatrix} \mathbf{r}^T & \mathbf{0}_{1 \times 3} \\ \mathbf{0}_{1 \times 3} & \mathbf{r}^T \end{bmatrix} \begin{bmatrix} \mathbf{A} \\ \mathbf{B} \end{bmatrix} \quad (32)$$

where

$$\mathbf{A}^T = \begin{bmatrix} \sin(\theta) \sin(\lambda) & \cos(\theta) \sin(\lambda) & 0 \\ -\cos(\theta) & -\sin(\theta) & 0 \end{bmatrix} \quad (33a)$$

$$\mathbf{B}^T = \begin{bmatrix} 0 & 0 & 0 \\ -\cos(\theta) \cos(\lambda) & \sin(\theta) \cos(\lambda) & -\sin(\lambda) \end{bmatrix} \quad (33b)$$

Then the expression can be written as  $\frac{d\Theta}{d\mathbf{v}^T}$

$$\frac{d\Theta}{d\mathbf{v}^T} = \begin{bmatrix} \frac{1}{1+\mathcal{X}^2} & 0 \\ 0 & \frac{1}{\sqrt{1-\mathcal{Y}^2}} \end{bmatrix} \begin{bmatrix} -(v_z \|\mathbf{v}\|^{-3} v_x) & -(v_z \|\mathbf{v}\|^{-3} v_y) & (\|\mathbf{v}^*\|^2 \|\mathbf{v}\|^{-3} v_x) \\ -(v_y \|\mathbf{v}^*\|^{-3} v_x) & (v_x^2 \|\mathbf{v}^*\|^{-3}) & 0 \end{bmatrix} \quad (34)$$

where  $\mathcal{X} = v_z / \|\mathbf{v}\|$  and  $\mathcal{Y} = v_y / \|\mathbf{v}^*\|$  and these terms are determined from differentiating Eq. (11b) and Eq. (11c). The quantity  $\|\mathbf{v}^*\| = \sqrt{v_x^2 + v_y^2}$  is used to define the magnitude of the  $x$  and  $y$  velocity vector. The covariance on the target plane given the linear transformation can be written as

$$\mathbf{P}_{\delta\delta} = \mathbf{F}(\boldsymbol{\mu}) \mathbf{P} \mathbf{F}(\boldsymbol{\mu})^T \quad (35)$$

where  $\mathbf{P}$  is the covariance at close approach, and  $\mathbf{P}_{\delta\delta}$  is the covariance on the target plane. Then under the linear transformation  $\mathbf{F}(\boldsymbol{\mu})$ , the pdf on the target plane can be written as a Gaussian distribution in the form

$$p(\boldsymbol{\delta}) = \mathcal{N}(\mathbf{B}(\boldsymbol{\mu}), \mathbf{P}_{\delta\delta}) \quad (36)$$

Then to calculate the probability of impact, the pdf for  $\boldsymbol{\delta}$  can be integrated over the Earth's effective disk on the target plane given by a disk center at the origin with radius  $b_e$ . The radius  $b_e$  on the other hand is a function of  $\|\mathbf{v}\|$  and  $\|\mathbf{r}\|$  as seen in Eq. (4) and Eq. (5) making  $b_e$  a function of  $p(\boldsymbol{\delta})$ . The first dependance is resolved by assuming  $\|\mathbf{r}\| > R_e$  as discussed in previously and the second dependance is resolved by assuming that  $\|\mathbf{v}\| = \|\mathbf{v}_\mu\|$  where  $\mathbf{v}_\mu$  is the velocity component of mean state  $\boldsymbol{\mu}$ . The effect of the uncertainty in  $b_e$  in calculating the impact probability is assumed to be small, this assumption on  $b_e$  is made for the rest of this paper. Furthermore, the state uncertainty is represented as a distribution of possible states the question arises of how to define the close approach. Under the EKF linear Gaussian assumption we consider the close approach point when the mean of the distribution makes a close approach, i.e  $\boldsymbol{\mu}$  is less then the close approach distance. The effect of this on the numerical results is discussed in the simulation results section.

## APPROXIMATE METHODS: UNSCENTED FILTER APPROACH

The basic difference between the EKF and the UKF results from the manner in which the state distribution of the nonlinear models is approximated. The UKF, introduced by Julier and Uhlmann<sup>17</sup> uses a nonlinear transformation called the scaled unscented transformation, in which the state probability distribution is represented by a set of weighted sigma points, which are used to parameterize the true mean and covariance of the state distribution. When the sigma points are propagated through the nonlinear system, the posterior mean and covariance is obtained up to the second order for any nonlinearity. The UKF algorithm is summarized in this section for discrete-time nonlinear models.

The original state vector is redefined in the UKF approach by augmenting the state vector to include noise variables, where the augmented state vector is defined by  $\mathbf{x}_k^a = [\mathbf{x}_k^T \mathbf{w}_k^T \mathbf{v}_k^T]^T$  and the augmented state vector has dimension  $n_a = n + q + l$ . All random variables in the UKF are assumed to be Gaussian random variables, therefore one can think of a joint distribution for the random variables, equivalent to the distribution of  $\mathbf{x}_k^a$ , defining multivariate Gaussian distribution given by  $p(\mathbf{x}_k^a) = p(\mathbf{x}_k, \mathbf{w}_k, \mathbf{v}_k)$ . The assumed statistics for  $\mathbf{w}_k$  and  $\mathbf{v}_k$  where discussed previously, then the joint distribution is approximated by  $p(\mathbf{x}_k, \mathbf{w}_k, \mathbf{v}_k) \sim \mathcal{N}(\mathbf{x}_k^a, \mathbf{P}^a)$ . The mean augmented vector  $\mathbf{x}_k^a$  can written as  $\boldsymbol{\mu}^a = [\boldsymbol{\mu}^T \mathbf{0}_{l \times 1}^T \mathbf{0}_{q \times 1}^T]^T$ , where  $\boldsymbol{\mu}$  is the state estimate. The covariance matrix,  $\mathbf{P}^a$ , for the joint distribution can be written as

$$\mathbf{P}^a = \begin{bmatrix} \mathbf{P} & \mathbf{P}^{xw} & \mathbf{P}^{xv} \\ \mathbf{P}^{wx} & \mathbf{Q} & \mathbf{P}^{wv} \\ \mathbf{P}^{vx} & \mathbf{P}^{vw} & \mathbf{R} \end{bmatrix} \quad (37)$$

Then the distribution is approximated as a set of symmetric selected scaled sigma points. The sigma points are selected such that they are zero-mean, but if the distribution has mean  $\boldsymbol{\mu}$ , then simply adding  $\boldsymbol{\mu}$  to each of the points yields a symmetric set of  $2n_a$  points having the same covariance as the initial Gaussian distribution.<sup>17</sup> The sigma points are selected to be along the principle axis direction of the Gaussian distribution  $p(\mathbf{x}_k^a)$  or along the eigenvector directions of  $\mathbf{P}_k^a$ . Then the augmented state vector and covariance matrix is constructed by

$$\boldsymbol{\sigma}_k \leftarrow 2N_a \text{ columns from } \sqrt{(n_a + \lambda)\mathbf{P}_k^a} \quad (38a)$$

$$\boldsymbol{\chi}_k^a(0) = \boldsymbol{\mu}_k \quad (38b)$$

$$\boldsymbol{\chi}_k^a(i) = \boldsymbol{\sigma}_k(i) + \boldsymbol{\mu}_k \quad (38c)$$

Therefore given a  $n_a \times n_a$  covariance matrix  $\mathbf{P}_k^a$ , a set of  $2n_a$  sigma points can be generated from the columns of the matrices  $\sqrt{(n_a + \lambda)\mathbf{P}_k^a}$ , where  $\sqrt{M}$  is shorthand notation for a matrix  $Z$  such that  $M = ZZ^T$ . Using the notation of the augmented state vector the sigma point vector can be written as

$$\boldsymbol{\chi}_k^a(i) = \begin{bmatrix} \boldsymbol{\chi}^x(i) \\ \boldsymbol{\chi}^w(i) \\ \boldsymbol{\chi}^v(i) \end{bmatrix} \quad (39)$$

Then given that these points are selected to represent the distribution of the augmented state vector, each sigma point is given a weight that preserves the information contained in the initial distribution:

$$W_0^{mean} = \frac{\lambda}{n + \lambda} \quad (40a)$$

$$W_0^{cov} = \frac{\lambda}{n + \lambda} + (1 - \alpha^2 + \beta) \quad (40b)$$

$$W_i^{mean} = W_i^{cov} = \frac{\lambda}{2(n + \lambda)} \quad (40c)$$

where  $\lambda = \alpha^2 n_a + \kappa - n_a$  includes scaling parameters. The constant parameter controls the size of the sigma point distribution and should be a small number  $0 \leq \alpha \leq 1$ , and  $\kappa$  provides an extra degree of freedom that is used to fine-tune the higher-order moments;  $\kappa = 3 - n_a$  for a Gaussian distribution, also  $\beta$  is a third parameter that further incorporates higher-order effects by adding the weighting of the zeroth sigma point to the calculation of the covariance; note  $\beta = 2$  is the optimal value for Gaussian distributions.

## Predictor

The state propagation and state uncertainty propagation is accomplished using the sigma points. The transformed set of sigma points are evaluated for each of the points by

$$\dot{\chi}^x(i, t) = \mathbf{f}(\chi^x(i, t), \chi^w(i, t)) \quad (41)$$

The predicted mean is given by

$$\boldsymbol{\mu}(t) = \sum_{i=0}^{2n} W_i^{mean} \chi^x(i, t) \quad (42)$$

The predicted covariance is given by

$$\mathbf{P}(t) = \sum_{i=0}^{2n} W_i^{cov} [\chi^x(i, t) - \boldsymbol{\mu}(t)][\chi^x(i, t) - \boldsymbol{\mu}(t)]^T \quad (43)$$

where  $\chi_k^x(i, t)$  is a weighted sigma point vector of the first  $n$  elements of the  $i^{\text{th}}$  augmented sigma point vector  $\chi^a$  and  $\chi^w$  is a weighted sigma point vector of the next  $q$  elements of  $\chi^a$ . Also  $\chi^v$  is a weighted sigma point vector of the  $l$  elements of the  $i^{\text{th}}$  augmented sigma point vector  $\chi^a$ , and  $W_i^{mean}$  is the weight for the mean and  $W_i^{cov}$  is the weight for the covariance, respectively.

## Corrector

Similarly, the predicted observation vector  $\hat{\mathbf{y}}_k$  at time step  $k$  and the innovation covariance  $\mathbf{P}_k^{vv}$  are calculated

$$\mathcal{Y}_k = \mathbf{h}_k(\chi_k^x, \chi_k^v) \quad (44a)$$

$$\bar{\mathbf{y}}_k = \sum_{i=0}^{2n} W_i^{mean} \mathcal{Y}_k(i) \quad (44b)$$

$$\mathbf{P}_k^{vv} = \sum_{i=0}^{2n} W_i^{cov} [\mathcal{Y}_k(i) - \bar{\mathbf{y}}_k][\mathcal{Y}_k(i) - \bar{\mathbf{y}}_k]^T \quad (44c)$$

Now, the filter gain is computed by

$$\mathcal{K}_k = P_k^{xy} (P_k^{vv})^{-1} \quad (45)$$

and the cross-correlation matrix is determined by

$$\mathbf{P}_k^{xy} = \sum_{i=0}^{2n} W_i^{cov} [\chi_k^x(i) - \boldsymbol{\mu}_k][\mathcal{Y}_k(i) - \bar{\mathbf{y}}_k]^T \quad (46)$$

The estimated state vector at current time step conditioned on the previous measurements up to and including the last time step is denoted as  $\hat{\mathbf{x}}_{k|k-1}$  and similar the covariance  $\mathbf{P}_{k|k-1}$  are given by

$$\boldsymbol{\mu}_{k|k} = \boldsymbol{\mu}_{k|k-1} + \mathcal{K}_k \mathbf{v}_{k+1} \quad (47)$$

$$\mathbf{P}_{k|k} = \mathbf{P}_{k|k-1} - \mathcal{K}_k \mathbf{P}_k^{vv} \mathcal{K}_k^T \quad (48)$$

It is noted that in the formulation of the UKF algorithm the correlated noise sources can be implemented efficiently without any modification of the filter algorithm. For the special case where both the process and measurement noise terms are purely additive, the computational complexity of the UKF can be reduced by adjusting the augmented state vector. For computational stability the matrix square root can be implemented by using a Cholesky factorization method that prevents the nonnegative covariance matrix.

### Target Plane Approximation

The UKF approach to propagating uncertainty can be applied to the target plane transformation by using the unscented transformation on the Gaussian distribution given by the UKF. Instead of linearizing about the nominal state vector, the unscented transformation approximates the distribution to a higher order of accuracy. Given the nonlinear target plane transformation in Eq. (10), the unscented transformation can be written as

$$\boldsymbol{\chi}^\delta = \mathbf{B}(\boldsymbol{\chi}^x) \quad (49)$$

The mean and covariance on the target plane are given by

$$\bar{\boldsymbol{\delta}} = \sum_{i=0}^{2n} W_i^{mean} \boldsymbol{\chi}^\delta(i) \quad (50a)$$

$$P_{\delta\delta} = \sum_{i=0}^{2n} W_i^{cov} [\boldsymbol{\chi}^\delta(i) - \bar{\boldsymbol{\delta}}][\boldsymbol{\chi}^\delta(i) - \bar{\boldsymbol{\delta}}]^T \quad (50b)$$

Under the unscented transformation, the pdf on the target plane can be written as a Gaussian distribution in the form

$$p(\boldsymbol{\delta}) = \mathcal{N}(\bar{\boldsymbol{\delta}}, P_{\delta\delta}) \quad (51)$$

where here  $\mathbf{P}_{\delta\delta}$  is the UKF covariance on the target plane. In contrast to the EKF target plane approach, for the UKF each sigma point is propagated to its own point of close-approach rather than the point where the mean of the distribution make its close-approach. Determining the close-approach time for each sigma point represents a more accurate approximation to the target plane transformation since the assumption of two body dynamics is made under the target plane transformation. If the uncertainty is large when the mean makes a close-approach there may be a region of non-negligible probability that may lie outside the sphere of influence of the Earth and the two body approach then becomes invalid. Therefore, each sigma point is propagated forward in time until the sigma point makes a close-approach where the target plane transformation is performed on this sigma point. All sigma points are propagated onto the target plane where a mean and covariance are calculated and the pdf is approximated by Eq. (51).

### APPROXIMATE METHODS: PARTICLE FILTER APPROACH

Particle filtering approaches are based on Monte Carlo methods, where a probability distribution is represented by set of randomly selected particles. Using the fact that the system in question can be solved for an individual set of initial conditions, the solution for a distribution of initial conditions are approximated by the solutions of a set of particles representing the initial distribution. Given  $N$  independent and identically distributed random samples  $\boldsymbol{x}^{(i)}$  drawn from  $p(\boldsymbol{x})$ ,  $i = 1, \dots, N$  the

distribution can be approximated by  $p(\mathbf{x}) \approx (1/N) \sum_{i=1}^N \delta(\mathbf{x} - \mathbf{x}^{(i)})$  and an arbitrary integral (or expectation) with respect to  $p(\mathbf{x})$  can be approximated by

$$\int \mathbf{f}(\mathbf{x})p(\mathbf{x})d\mathbf{x} \approx \frac{1}{N} \sum_{i=1}^N \mathbf{f}(\mathbf{x}^{(i)}) \quad (52)$$

Perfect Monte Carlo sampling assumes the samples are drawn directly from the distribution  $p(\mathbf{x})$  and that there are enough particles to represent the mass of the distribution. It can be shown that as  $N_a \rightarrow \infty$ , the approximation given by Eq. (52) approaches the true density.<sup>18</sup> In the case of the Particle filter each particle is assigned a weight,  $w^{(i)} \propto p(\mathbf{x}^{(i)})$ , which represents the probability of that particle occurring. Then the weights are normalized such that  $\sum_i^N w^{(i)} = 1$ . A particle filter involves four steps, namely, prediction, update (correction), resampling and regularization (roughening), all of these steps constitute a filter cycle.

### Predictor

The sets of particles and their associated weights representing the pdf at  $t_k$  and  $t_{k+1}$  are denoted by  $\{\mathbf{x}_k^{(i)}, w_k^{(i)}\}$  and  $\{\mathbf{x}_{k+1}^{(i)}, w_{k+1}^{(i)}\}$ , respectively, where  $i = 1, \dots, N$ . The particles at time  $t_k$  are propagated through the following equation with their weights unchanged:

$$\hat{\mathbf{x}}^{(i)} = \mathbf{f}(\mathbf{x}^{(i)}, \mathbf{w}^i) \quad (53)$$

Then the particle at time  $t_{k+1}$ ,  $\{\mathbf{x}_{k+1}^{(i)}, w_{k+1}^{(i)}\}$ , represents the forecast pdf, where  $N$  samples  $\mathbf{w}^{(i)}$  of the process noise are drawn according to  $p(\mathbf{w})$ , denoted by  $\mathbf{w}_k^{(i)} \sim p(\mathbf{w}_k)$ ,  $i = 1, \dots, N$ , is the normalized weight of the particle. The process noise  $\mathbf{w}$  and the measurement noise  $\mathbf{v}$  are assumed to be zero-mean white noise sequences. Although no Gaussian assumptions are needed, the distributions of the mutually independent  $\mathbf{x}_o$ ,  $\mathbf{w}$ , and  $\mathbf{v}$ , denoted by  $p(\mathbf{x}_o)$ ,  $p(\mathbf{w})$  and  $p(\mathbf{v})$ , respectively, are assumed to be known and Gaussian for this work. Then, the posterior density at  $k$  can be approximated as

$$p(\mathbf{x}(t)) \approx \sum_{i=1}^i w^i \delta(\mathbf{x}(t) - \mathbf{x}^i(t)) \quad (54)$$

where  $\delta(\cdot)$  represents the Dirac delta function, which returns one for an argument of zero and zero otherwise. Equation (54) represents a discrete weighted approximation to the true posterior.

### Corrector

When measurements are made available, the pdf is updated by updating the weights of each particle using the likelihood of the measurement given each particle. At the update step the weight associated with each particle is updated based on the likelihood function  $w_{k+1}^{(i)} = w_k^{(i)} p(\tilde{\mathbf{y}}_k | \mathbf{x}_k^{(i)})$ : where  $w_{k+1}^{(i)}$  denotes the unnormalized weights. If additive noise is considered the likelihood function has a simple form:  $p(\tilde{\mathbf{y}}_{k+1} | \mathbf{x}^{(i)}) = p(\tilde{\mathbf{y}}_k - \mathbf{h}(\mathbf{x}_k^{(i)}))$ . Then weight update for each particle is based on the likelihood function and given by

$$w_k^{(i)} = w_{k-1}^{(i)} p(\tilde{\mathbf{y}}_k | \mathbf{x}_{k-1}^{(i)}) \quad (55a)$$

$$w_k^{(i)} = \frac{w_k^{(i)}}{\sum_{i=1}^N w_k^{(i)}} \quad (55b)$$

where the likelihood function  $p(\tilde{\mathbf{y}}_k | \mathbf{x}_k^{(i)})$  depends on the noise process of the observation directly.

## Resampling and Regularization

The variance associated with the weights in sequential importance sampling can only increase over time and eventually all but one particle will have negligible weight.<sup>18</sup> To overcome this degeneracy problem resampling is used to discard obsolete particles with small weights and multiply particles with large weights.<sup>19</sup> The resampling procedure starts by drawing samples  $N$  times from  $\{\mathbf{x}_{k+1}^{(i)}, w_{k+1}^{(i)}\}$  to obtain  $N$  equally weighted particles,  $\{\mathbf{x}_{k+1}^{(i)}, 1/N\}$ .

Since resampling duplicates the particles with large weights, generating many identical particles may greatly decrease the number of distinct particles, resampling is usually followed by a regularization step. The regularization step adds small noise to the resampled particles to increase particle diversity.<sup>19</sup> A small independent jitter drawn from a Gaussian distribution is added to the identical particles to increase diversity.

## Target Plane

The PF approach to propagating uncertainty can be applied to the target plane transformation to represent the uncertainty on the target plane. Given the nonlinear target plane transformation in Eq. (10) and the asteroid's initial distribution  $p(\mathbf{x})$  represented by a set of weighted particles, the probability density of the asteroid on the target plane can be written as

$$p(\boldsymbol{\delta}) = \sum_{i=0}^N w_i \delta(\mathbf{B}(\mathbf{x}) - \mathbf{B}(\mathbf{x}^{(i)})) \quad (56)$$

where the weights are unchanged from those of the initial particle set. In a similar manner to the unscented transformation approach, each particle is propagated to its own point of close-approach rather than to the point where the mean of the distribution makes its close-approach.

## SIMULATION RESULTS

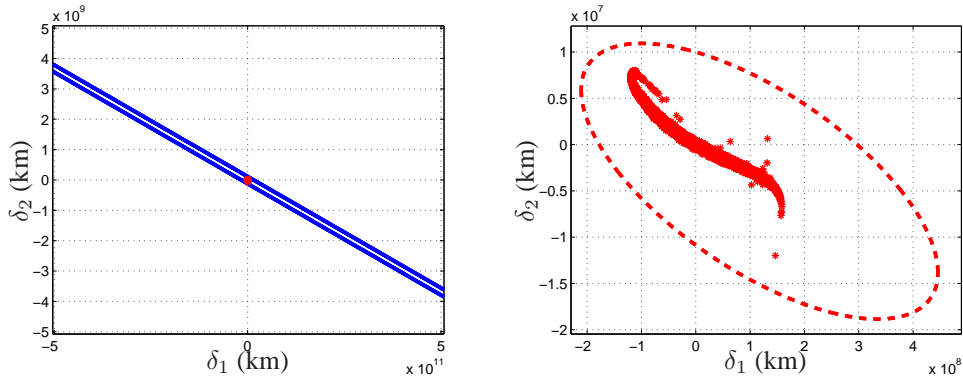


**Figure 2. Target Plane Propagated Densities, Target Plane  $3\sigma$  to scale on left and Target Plane  $3\sigma$  Zoomed in on right.**

In this section the performance of the proposed nonlinear filters, the EKF, UKF, and PF, is demonstrated through simulation examples using a realistic near-Earth asteroid orbit and initial uncertainty. The asteroid under consideration has the orbit parameters given in Table 1 for an epoch JD 2453736.5. The initial error covariance  $\mathbf{P}_o$  is theoretically an expectation  $E\{(\mathbf{x}_o - \hat{\mathbf{x}}_o)(\mathbf{x}_o - \hat{\mathbf{x}}_o)^T\}$ ,

**Table 1. Initial Uncertainty Used for Simulations for Epoch JD 2453736.5**

|          |       | Initial Estimate | Initial Variances         |
|----------|-------|------------------|---------------------------|
| $a$      | (AU)  | 0.922            | $0.96 \times 10^{-8}$     |
| $e$      |       | 0.191            | $0.297 \times 10^{-7}$    |
| $i$      | (Deg) | 3.331            | $0.7966 \times 10^{-6}$   |
| $\Omega$ | (Deg) | 204.446          | $0.425720 \times 10^{-4}$ |
| $\omega$ | (Deg) | 126.364          | $0.422150 \times 10^{-4}$ |
| $M$      | (Deg) | 151.057          | $0.10854 \times 10^{-5}$  |

where  $\mathbf{x}_o$  is the initial estimate vector given by the values in Table 1. The initial error covariance adopted is a diagonal matrix representing uncertainty in a hypothetical orbit determination performed on asteroid under consideration. The diagonal elements of the initial error covariance are given by the values listed in Table 1. The process noise matrix  $\mathbf{Q}$  in all three filters is assumed to be  $0_{3 \times 3}$ , following a traditional approach for orbit estimation.

The system dynamic equations consist of the  $N$ -body motion given by Eq. (1) without process noise. All dynamic and matrix differential equations are numerically integrated by using a fourth-order RungeKutta algorithm. For the simulation the position and velocity are used as states and the initial conditions are converted to cartesian coordinates. The three filter approaches are also applied in cartesian coordinates. In the simulation studies the initial position and velocity estimates for the EKF, UKF, and PF are assumed to be given by values in Table 1. The initial pdfs are approximated as Gaussian pdfs for the three filters (in the case of the PF the initial particles are sampled from this distribution). The asteroid under consideration has a close-approach at JD 2462237.63963 (or 2029 April 11) and for this approach as the asteroid enters the Earth’s sphere of influence, with respect to the Sun, the target plane transformation is applied.

The EKF uncertainty is propagated by integrating Eq. (19) using the covariance values from Table 1 as an initial condition until close-approach. Then once the mean orbit enters the Earth’s sphere of influence, Eq. (35) is used to propagate the pdf onto the target plane at close-approach. For the UKF parameters,  $\beta = 3$  is set to capture the higher-order terms in the Taylor-series expansion and  $\alpha = 10^{-3}$  is chosen to make the sample distance independent of the state size. Samples from the initial Gaussian pdf are taken for the PF approach and these samples are propagated using the system model Eq. (1) keeping their weights constant considering that no additional measurements are used. Then as each particle enters the Earth’s sphere of influence the target plane transformation is applied using Eq. (11a). Simulation results are presented using the  $3\sigma$  values for the EKF and UKF plotted along with the PF particles over the times span leading up the close-approach. Four times are plotted: 2005 (Figure 3), 2010 (Figure 4), 2015 (Figure 5), and just before encounter at 2029 (Figure 6).

The initial pdfs for the three filters is presented in Figure 3. The PF’s initial pdf is considered to be 20,000 points sampled from the initial Gaussian distribution. The red points in Figure 3 represent the particles from the PF and the red line represents the  $3\sigma$  bounds for the Gaussian distribution assumed for the UKF. Similarly the  $3\sigma$  bounds for the Gaussian distribution assumed for the EKF is plotted in blue line coinciding with the UKF  $3\sigma$  bound initially. Then for the EKF the mean is propagated until it enters the sphere of influences, then the covariance is propagated linearly onto

the target plan. For UKF and PF each sigma point and particle is propagated until it enters the sphere of influences, then the target plane transformation is applied on each point. Figures 3-6 show the three filters plotted progressively through the propagation period.

It can be noted that initially the performance of the three nonlinear filter approaches are very similar but, as expected, as the propagation time increases the EKF over-estimated the covariance of the distribution in comparison to the PF, especially seen in Figure 6. Although the UKF also over-estimated the covariance of the distribution in comparison to the PF it consistently outperformed the EKF throughout the propagation period. After all three approaches are propagated to 2029 the target plane transformation is applied. The PF particles are shown on the target plane along with the  $3\sigma$  bound of the EKF and UKF in Figure 2. Here the manner that the EKF approximates the target plane transformation led to an over-estimate of the covariance on the target plane. Since uncertainty right before the target approximation is large the linearization is about a large region and the two body approximation is also about a large region as well. Since in the EKF there exists regions within the linearization region that is outside the Earth's sphere of influence the deflection of these points by the Earth gravity would be small and therefore these regions would lie far from the Earth on the target plane. This is seen in the fact that the EKF  $3\sigma$  bound is very large and elongated in comparison to the PF. The UKF in this case performed very well since the manner that the covariance is propagated allows for each sigma point to enter the sphere of influence independently, a more accurate representation of the target plane uncertainty is found with the UKF.

The PF represents the most accurate approach. For detail studies this method is preferred over all others but the computational cost in very high with this approach. The simulation of the PF presented here took approximately 5 hours to finish while the EKF and UKF where both an order of magnitude faster, only taking 45-60 sec. The benefit of the EKF and UKF is that these approach can give initial estimates of impact probability with low computational cost, and highlight potential threats that need to be studied in more detail with a PF approach. Since the number of NEOs that need to classified is very large, a computation inexpensive threat classification approach is appealing.

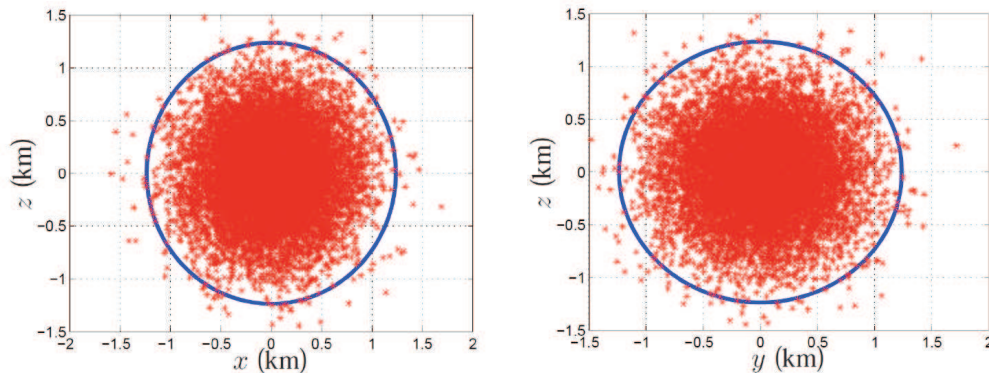


**Figure 3. Uncertainty in initial position at 2005, uncertainty in the z and y components on the right and uncertainty in the z and x components on the left.**

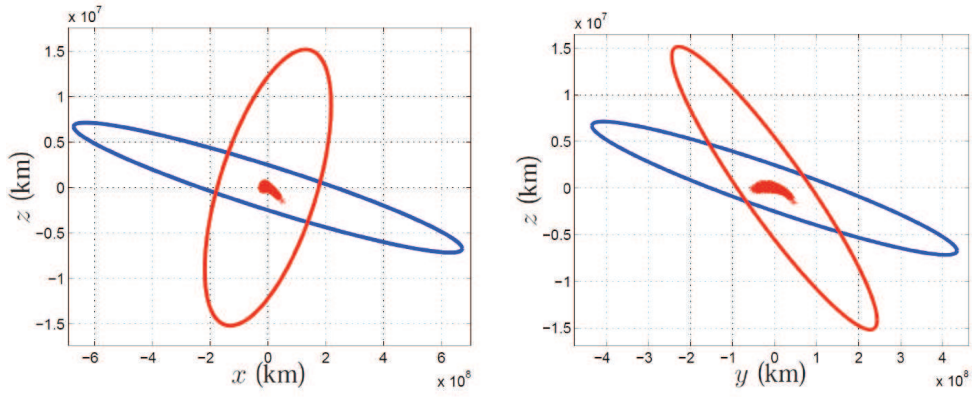


Figure 4. Uncertainty in position at 2010, uncertainty in the  $z$  and  $x$  components on the right and uncertainty in the  $z$  and  $y$  components on the left.

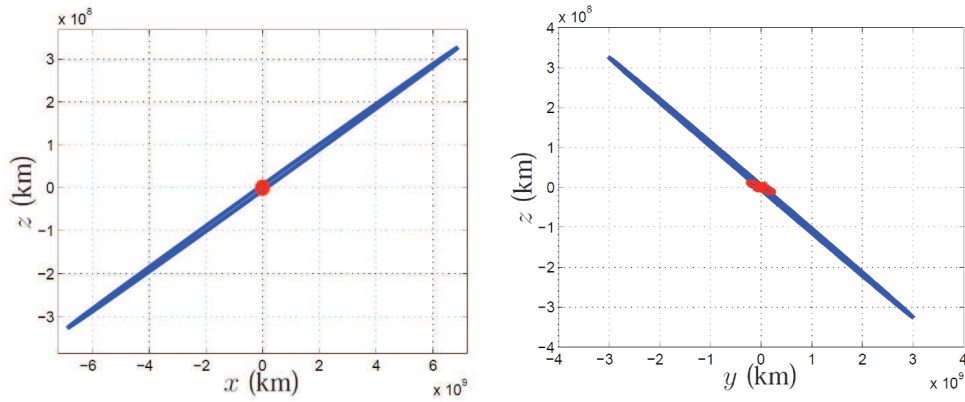


Figure 5. Uncertainty in position at 2015, uncertainty in the  $z$  and  $x$  components on the right and uncertainty in the  $z$  and  $y$  components on the left.

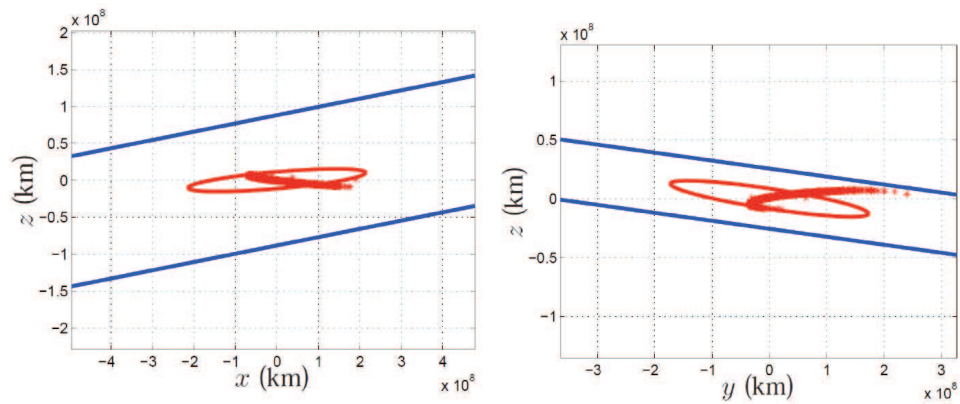


Figure 6. Uncertainty in position at 2029, uncertainty in the  $z$  and  $x$  components on the right and uncertainty in the  $z$  and  $y$  components on the left.

## CONCLUSION

The impact probability estimation problem has been considered for three nonlinear sequential estimators, the Extended Kalman Filter (EKF), the Unscented Kalman Filter (UKF) and the Particle Filter (PF). All three filters studied were considered for estimating the impact probability of an asteroid given initial orbit uncertainty. The results show that initially the performance of the three nonlinear filter approaches were very similar but, as expected, as the propagation time increases the linear assumption made by the EKF was incorrect, resulting in a large covariance for the EKF compare to the PF results. The UKF provides good performance over most of the time span, and the UKF covariance captures evolution of uncertainty reasonably well. Finally the three filter approaches were used to propagate the encounter uncertainty onto the target plane. The pdf on the target plane was shown and again the linear assumption of the EKF fail due the large state covariance. The UKF pdf very well approximates the PF distribution, but still failed to capture the tail of the full distribution.

## REFERENCES

- [1] G. W. Wetherill and J. G. Williams, "Origin of Differentiated Meteorites and Distribution of the Elements," *Proceedings of the Second Symposium*, Vol. 34, May 1979.
- [2] J. Wisdom, "Meteorites May Follow a Chaotic Route to Earth," *Nature*, Vol. 315, June 1985, pp. 731–733.
- [3] M. Carpino, A. Milani, and S. R. Chesley, "Error Statistics of Asteroid Optical Astrometric Observations," *ESSAI*, Vol. 166, December 2003, pp. 248–270.
- [4] E. Bowell, J. Virtanen, K. Muinonen, and A. Boattini, "Asteroid Orbit Computation," *Asteroids III*, Vol. Univ. of Arizona, Tucson, Jan 2002, pp. 27–43.
- [5] E. J. pik, *Interplanetary Encounters: Close-Range Gravitational Interactions*, p. 155. New York: Elsevier, 2006.
- [6] P. W. Chodas and D. K. Yeomans, "The Orbital Motion and Impact Circumstances of Comet Shoemaker-Levy 9," *Proceedings of the Space Telescope Science Institute Workshop*, Vol. 31, May 1996, pp. 1–30.
- [7] P. W. Chodas and D. K. Yeomans, "Could Asteroid 1997 XF11 Collide with Earth after 2028?," *American Astronomical Society, DDA meeting*, Vol. 31, Jan 1999, p. 07.03.
- [8] A. Milani, S. R. Chesley, A. Boattini, and G. B. Valsecchi, "Virtual Impactors: Search and Destroy," *Icarus*, Vol. 145, May 1999, pp. 12–24.
- [9] H. Risken, *The Fokker-Planck Equation: Methods of Solution and Applications*. Springer, 1989, 1-12, 32-62.
- [10] M. Kumar, P. Singla, S. Chakravorty, and J. L. Junkins, "The Partition of Unity Finite Element Approach to the Stationary Fokker-Planck Equation," *2006 AIAA/AAS Astrodynamics Specialist Conference and Exhibit*, Keystone, CO, Aug. 21-24, 2006.
- [11] M. Kumar, S. Chakravorty, and J. L. Junkins, "A Semianalytic Meshless Approach to the Transient Fokker-Planck Equation with Application to Hybrid Systems," *Conference on Decision and Control*, New Orleans, LA, July 11-13, 2007.
- [12] A. Doucet, N. d. Freitas, and N. Gordon, *Sequential Monte-Carlo Methods in Practice*. Springer-Verlag, April 2001, 6-14.
- [13] R. N. Iyengar and P. K. Dash, "Study of the Random Vibration of Nonlinear Systems by the Gaussian Closure Technique," *Journal of Applied Mechanics*, Vol. 45, 1978, pp. 393–399.
- [14] J. B. Roberts and P. D. Spanos, *Random Vibration and Statistical Linearization*. Wiley, 1990, 122-176.
- [15] T. Lefebvre, H. Bruyninckx, and J. D. Schutter, "Kalman Filters of Non-Linear Systems: A Comparison of Performance," *International journal of Control*, Vol. 77, No. 7, 2004, pp. 639–653.
- [16] R. E. Kalman, "A New Approach to Linear Filtering and Prediction Problems," *Transactions of the ASME Journal of Basic Engineering*, Vol. 82, 1960, pp. 35–45. Series D.
- [17] S. Julier and J. Uhlmann, "Unscented Filtering and Nonlinear Estimation," *Proceedings of the IEEE*, Vol. 92, No. 3, 2004, pp. 401–422.
- [18] I. H. Sloan and H. Woniakowski, "When Are Quasi-Monte Carlo Algorithms Efficient for High Dimensional Integrals?," *Journal of Complexity*, 1998, pp. 1–33.

- [19] P. Djuric and S. Godsill, "Special Issue on Monte Carlo Methods for Statistical Signal Processing," *IEEE Transactions on Signal Processing*, Vol. 50, No. 2, 2002.